International Journal of Fluid Mechanics & Thermal Sciences
2020; 6(3): 70-78
http://www.sciencepublishinggroup.com/j/ijfmts
doi: 10.11648/j.ijfmts.20200603.11
ISSN: 2469-8105 (Print); ISSN: 2469-8113 (Online)

Review Article

Peristaltic Flow with Heat Transfer on Sisko Fluid in a Ciliated Arteries

Bothaina Mohamed Agoor[1, *], Mohamed Eissa Sayed-Ahmed[2], Heba Alam[1]

[1]Department of Mathematics, Faculty of Science, Fayoum University, Fayoum, Egypt

[2]Department of Engineering Mathematics and Physics, Faculty of Engineering, Fayoum University, Fayoum, Egypt

Email address:
bma00@fayoum.edu.eg (B. M. Agoor)

[*]Corresponding author

To cite this article:
Bothaina Mohamed Agoor, Mohamed Eissa Sayed-Ahmed, Heba Alam. Peristaltic Flow with Heat Transfer on Sisko Fluid in a Ciliated Arteries. *International Journal of Fluid Mechanics & Thermal Sciences*. Vol. 6, No. 3, 2020, pp. 70-78. doi: 10.11648/j.ijfmts.20200603.11

Received: June 30, 2020; **Accepted**: July 24, 2020; **Published**: August 10, 2020

Abstract: The flow of blood through arteries is an important physiological problem. In the present investigation, we carried out to study the peristaltic of non-Newtonian incompressible blood flow with heat transfer through ciliated arteries. The blood flow is characterized by the generalized Sisko model. The nonlinear partial differential equations of the problem are simplified by using an approximation of long wavelength and low Reynolds number. The differential equations are solved analytically by using the perturbation method .We find that Sisko fluid parameter and the power index effects the behavior of the velocity where the velocity increase in the arteries then decreases near the wall, but the Sisko parameter give opposite behavior where the velocity decrease then increases near the wall of arteries. The velocity increase in arteries with the increase of cilia length and elliptic path. The temperature profile increases then decreases near the wall of arteries with the increase of power index, Sisko fluid parameter and Grashof number, while the temperature decrease then increase near the wall with increase of Sisko parameter. The effect of increase in the cilia length give an increase of the temperature. The pressure gradient increases with the increase of power index and elliptic path, while the pressure gradient decrease with an increase of elliptic path, Sisko parameter. The pressure gradient increases and decreases in a different interval with the increase the cilia length. Our results are illustrated through a set of Figures.

Keywords: Sisko Fluid Model, Perturbation Method, Peristaltic Flow, Non-newtonian Fluid and Heat Transfer

1. Introduction

In fluid mechanics, Cilia are small hair-like structures, those projects from the free surface of certain cells and play important role in many psychological processes such as locomotion, alimentation, sensory perception [1], respiration, reproduction, and development [2] in a wide range of eukaryotes including human. There are two types of cilia motile and non-motile cilia, motile cilia are important for clearance of mucosa (airways), transport of oocytes (fallopian tubes) and circulation of cerebrospinal fluid (brain) [3] and are found in groups. In the adult human body, epithelial cells with motile cilia are highly rich in airways, reproductive tracts, and specific brain regions [4]. Whereas, primary cilia or (non-motile cilia) are usually found only one at a time on cell. Examples of non- motile cilia can be found in human sensory organs such as the eye and the nose. Some various studies about cilia transport have been achieved by [5-10] Discuss the effects of viscous Nanofluid due to ciliary motion in an annulus. [11] Have studied a metachronal wave analysis for non-Newtonian fluid inside a symmetrical channel with ciliated walls. Cilia walls influence on peristaltically induced motion of magneto-fluid through a porous medium at moderate Reynolds number has studied by [12]. Ciliary bands are used to produce feeding currents that draw the food particles toward the mouth of the organism for feeding [13, 14]. Cilia facilitate organism swimming [14, 15]. Oscillatory wavy walled (peristalsis) is a form of fluid transport induced by a progressive wave of area contraction and expansion of the length of a distensible tube containing fluid. Peristalsis plays important phenomena in the transport of biofluid it is well known to physiologists to be one of the major mechanisms for fluid transport in many biological systems. Peristaltic is

characterized by swap reduction and leisure. Which pushes foodstuff in the course of the digestive area towards its let go at the anus Peristaltic flow occurs widely in the functioning of the ureter, food mixing and chime movement in the intestine, movement of ovum in the fallopian tube, the transport of the spermatozoa in the cervical canal, transport of cilia and circulation of blood in small blood vessels. Also, peristalsis involves in many industrial and biomedical applications like sanitary fluid transport, blood pumps in the heart-lung machine and transport of corrosive fluid where the contact fluid with the machinery parts is prohibited the problem of the peristaltic transport has attracted the attention of many investigators. The idea of peristaltic transport in a mathematical point of view was first coined by Latham [16]. Peristaltic transport has been studied under various conditions by using different assumptions like long wavelength or small amplitude ratio. Srivastava and Saxena [17] studied a two-fluid model of non-Newtonian blood flow induced by peristaltic waves. Sucharitha et al. [18] described the peristaltic flow of non-Newtonian fluids in an asymmetric channel with a porous medium. The peristaltic flow of micropolar fluid in an asymmetric channel with permeable walls is discussed by Sreenadh et al. [19, 20] Discuss the effect of slip and heat transfer on the peristaltic transport of Jeffery fluid in a vertical asymmetric porous channel. [21] Created MHD peristaltic transportation of conducting blood flow with a porous medium through an inclined coaxial vertical channel. [22] Have studied peristaltic transport of a couple stress fluids some applications to hemodynamics. The peristaltic flow of a Sisko fluid over a convectively heated surface with viscous dissipation is investigated by [23]. Mathematical modeling of Sisko fluid flow through a stenosed artery discussed by [24, 25] Study the boundary layer equations and lie group analysis of a Sisko fluid. [26] Investigated the influences of the peristaltic flow of Sisko fluid in a uniform inclined tube. [27] Discussed the peristaltic Sisko nanofluid in an asymmetric channel. The focus of the study of the peristaltic flow of Sisko fluid with heat transfer on ciliated arteries is to obtaining details analytical solutions using the perturbation method. The flow is considered to be obeying the constitutive equation of Sisko's model fluid, this describes the proposed solution methodologies for the governing systems of non-linear partial differential equations, this presented the analytical results and discussion, finally the paper is concluded with a discussion of the results.

2. Formulation of the Problem

Consider the peristaltic flow of an incompressible Sisko fluid in ciliated arteries with heat transfer. The geometry of the problem is shown in Figure 1. The fluid under the action of a ciliary that generates a metachronal wave. The flow propagating with constant speed c along the walls of the arteries whose inner surface is ciliated. We are considering the cylindrical coordinate system $\left(\overline{R},\overline{Z}\right)$, where $\overline{Z}$ axis lies along the centerline of the arteries and $\overline{R}$ is transverse to it. The flow of the fluid are described in two coordinate systems, one is fixed in the space $\left(\overline{R},\overline{Z}\right)$ and the other is $\left(\overline{r},\overline{z}\right)$ moving with the same speed c as the wave moves in the $\overline{z}$ - direction the transformation between the two coordinate systems are:

$$\overline{r}=\overline{R},\ \overline{z}=\overline{Z}-ct,\ \overline{u}=\overline{U},\ \overline{w}=\overline{W}-c, \tag{1}$$

Where $\left(\overline{u},\overline{w}\right)$ and $\left(\overline{U},\overline{W}\right)$ are the velocity components in the moving and fixed frame. The geometry of the wall surface is defined as (in fixed frame)

$$H\left(\overline{Z},t\right)=a+a\varepsilon\cos\frac{2\pi}{\lambda}\left(\overline{Z}-ct\right) \tag{2}$$

Where a is the radius of the tube, ε is the cilia length, λ is the wavelength, c is the wave velocity of the metachronal wave and t is the time. The cilia tips moving in elliptical path which can be represented mathematically in the form.

$$F\left(Z,t\right)=Z_0+\alpha\varepsilon a\sin\frac{2\pi}{\lambda}\left(\overline{Z}-ct\right) \tag{3}$$

Where Z_0 is a reference position of the cilia and α is a measure of the eccentricity of the elliptic path. The equations for conservation of mass, momentum and heat transfer can be written as

$$\frac{\partial\overline{U}}{\partial\overline{R}}+\frac{\overline{U}}{\overline{R}}+\frac{\partial\overline{W}}{\partial\overline{Z}}=0 \tag{4}$$

$$\rho\left(\frac{\partial\overline{U}}{\partial\overline{t}}+\overline{U}\frac{\partial\overline{U}}{\partial\overline{R}}+\overline{W}\frac{\partial\overline{U}}{\partial\overline{Z}}\right)=-\frac{\partial\overline{P}}{\partial\overline{R}}+\frac{1}{\overline{R}}\frac{\partial}{\partial\overline{R}}\left(\overline{R}\overline{S}_{\overline{R}\overline{R}}\right)+\frac{\partial\overline{S}_{\overline{R}\overline{Z}}}{\partial\overline{Z}}-\frac{\overline{S}_{\overline{\theta}\overline{\theta}}}{\overline{R}}, \tag{5}$$

$$\rho\left(\frac{\partial\overline{W}}{\partial\overline{t}}+\overline{U}\frac{\partial\overline{W}}{\partial\overline{R}}+\overline{W}\frac{\partial\overline{W}}{\partial\overline{Z}}\right)=-\frac{\partial\overline{P}}{\partial\overline{Z}}+\frac{1}{\overline{R}}\frac{\partial}{\partial\overline{R}}\left(\overline{R}\overline{S}_{\overline{R}\overline{Z}}\right)+\frac{\partial\overline{S}_{\overline{Z}\overline{Z}}}{\partial\overline{Z}} \tag{6}$$

$$\rho c_p\left(\frac{\partial\overline{\mathrm{T}}}{\partial\overline{t}}+\overline{U}\frac{\partial\overline{\mathrm{T}}}{\partial\overline{R}}+\overline{W}\frac{\partial\overline{\mathrm{T}}}{\partial\overline{Z}}\right)=k\left(\frac{1}{\overline{R}}\frac{\partial}{\partial\overline{R}}\left(\overline{R}\frac{\partial\overline{\mathrm{T}}}{\partial\overline{R}}\right)+\frac{\partial^2\overline{T}}{\partial Z^2}\right)+\overline{S}_{\overline{R}\overline{R}}\frac{\partial\overline{U}}{\partial\overline{R}}+\overline{S}_{\overline{R}\overline{Z}}\left(\frac{\partial\overline{U}}{\partial\overline{Z}}+\frac{\partial\overline{W}}{\partial\overline{R}}\right)+\overline{S}_{\overline{Z}\overline{Z}}\frac{\partial\overline{W}}{\partial\overline{Z}}+\overline{S}_{\overline{\theta}\overline{\theta}}\frac{\overline{U}}{\overline{R}}, \tag{7}$$

Where ρ is the density, t represents the time, c_p is the specific heat at constant volume, k is the thermal conductivity, $\overline{P}$ is the pressure, $\overline{T}$ is the temperature of fluid and $\overline{S}$ is the extra stress tensor of Sisko fluid is given by

$$\overline{S}=\left[a_1+b_1\left(\sqrt{\frac{1}{2}tr\left(A_1\right)^2}\right)^{n-1}\right]A_1 \tag{8}$$

Where A_1 is the rate of deformation tensor, a_1, b_1 and n are the physical constants of Sisko fluid model, the Rivlin- Erickson tensor is defined as follows:

$$A_1=\underline{L}+\underline{L}^T,\ \underline{L}=grad\ \ \overline{v} \tag{9}$$

The corresponding boundary conditions are:

$$\left.\begin{aligned}&\frac{\partial\overline{W}}{\partial\overline{R}}=0 \qquad ,\frac{\partial T}{\partial R}=0 \qquad at \qquad \overline{R}=0\\&\overline{W}=\frac{-2\pi\varepsilon a\alpha c}{\lambda}\cos\frac{2\pi}{\lambda}\left(\overline{Z}-c\overline{t}\right) \quad ,T=T_0 \quad at \qquad \overline{R}=H\end{aligned}\right\} \tag{10}$$

Let us introduce the following dimensionless:

$$\left.\begin{aligned}&r=\frac{\overline{r}}{a},\ z=\frac{\overline{z}}{a},\ u=\frac{\overline{u}}{c\delta},,\ w=\frac{\overline{w}}{c},\ R_e=\frac{\rho ca}{\mu},\\&h=\frac{H}{a}=1+\varepsilon\cos 2\pi z,\ S_{ij}=\frac{a}{\mu c}\overline{S}_{ij},\ a_s=\frac{a_1c}{a},\ b_s=b_1\left(\frac{c}{a}\right)^n,\\&\delta=\frac{a}{\lambda},\ t=\frac{c}{\lambda}\overline{t},\ \theta=\frac{\overline{T}-T}{T_1-T_0},\ G_r=\frac{\mu c^2}{k\left(T_1-T_0\right)},p=\frac{a^2}{\mu c\lambda}\overline{p}\end{aligned}\right\} \tag{11}$$

Making use of equations (1) and (11), the governing equations (4) to (7) take the form

$$\frac{\partial u}{\partial r}+\frac{u}{r}+\frac{\partial w}{\partial z}=0, \tag{12}$$

$$R_e\delta^3\left(u\frac{\partial u}{\partial\overline{r}}+w\frac{\partial u}{\partial z}\right)=-\frac{\partial p}{\partial r}+\frac{\delta}{r}\frac{\partial}{\partial r}\left(rS_{rr}\right)+\delta^2\frac{\partial S_{rz}}{\partial z}-\delta\frac{S_{\theta\theta}}{r}, \tag{13}$$

$$R_e\delta\left(u\frac{\partial w}{\partial\overline{r}}+w\frac{\partial w}{\partial z}\right)=-\frac{\partial p}{\partial z}+\frac{1}{r}\frac{\partial}{\partial r}\left(rS_{rz}\right)+\delta^2\frac{\partial S_{zz}}{\partial z} \tag{14}$$

$$\rho c_p\delta\left(T_1-T_0\right)\left(u\frac{\partial\theta}{\partial r}+w\frac{\partial\theta}{\partial z}\right)=\frac{k\left(T_1-T_0\right)}{a_sc}\left(\frac{1}{r}\frac{\partial}{\partial r}\left(r\frac{\partial\theta}{\partial r}\right)+\delta^2\frac{\partial^2\theta}{\partial z^2}\right)+\delta S_{rr}\frac{\partial u}{\partial r}+\overline{S}_{rz}\left(\frac{\partial w}{\partial r}+\delta^2\frac{\partial u}{\partial z}\right)+\delta\ \ S_{zz}\frac{\partial w}{\partial z}+\delta\ \ S_{\theta\theta}\frac{u}{r}, \tag{15}$$

With the boundary conditions

$$\left.\begin{aligned}&\frac{\partial w}{\partial r}=0 \qquad , \quad \frac{\partial\theta}{\partial r}=0 \qquad at \qquad r=0\\&w=-1-2\pi\alpha\varepsilon\delta\cos\left(2\pi z\right) \quad , \ \theta=1 \qquad at \qquad r=h\end{aligned}\right\} \tag{16}$$

Where

$$\left.\begin{aligned} S_{rr} &= \frac{2c\delta}{a}\left[a_1 + b_1\left|\frac{1}{2}t_r A^2\right|^{\frac{n-1}{2}}\right]\left(\frac{\partial u}{\partial r}\right),\ S_{rz} = \frac{c}{a}\left[a_1 + b_1\left|\frac{1}{2}t_r A^2\right|^{\frac{n-1}{2}}\right]\left(\delta^2\frac{\partial u}{\partial z} + \frac{\partial w}{\partial r}\right), \\ S_{zz} &= \frac{2c\delta}{a}\left[a_1 + b_1\left|\frac{1}{2}t_r A^2\right|^{\frac{n-1}{2}}\right]\left(\frac{\partial w}{\partial r}\right),\ S_{\theta\theta} = \frac{2c\delta}{a}\left[a_1 + b_1\left|\frac{1}{2}t_r A^2\right|^{\frac{n-1}{2}}\right]\left(\frac{u}{r}\right), \\ \left|\frac{1}{2}t_r A^2\right| &= \left(\frac{c}{a}\right)^2\left[2\delta^2\left(\frac{\partial u}{\partial r}\right)^2 + 2\delta^2\left(\frac{\partial w}{\partial z}\right)^2 + 2\delta^2\left(\frac{u}{r}\right)^2 + \left(\delta^2\frac{\partial u}{\partial z} + \frac{\partial w}{\partial r}\right)^2\right]. \end{aligned}\right\} \tag{17}$$

By using the long-wavelength approximation $\delta\langle\langle 1$ and small Reynolds number $R_e\langle\langle 1$, we neglecting the terms containing δ, R_e and higher order, then equations (13) - (15) take the form.

$$0 = \frac{\partial p}{\partial r} \tag{18}$$

$$0 = -\frac{\partial p}{\partial z} + \frac{1}{r}\frac{\partial}{\partial r}\left(r\left(a_s\frac{\partial w}{\partial r} + b_s\left(\frac{\partial w}{\partial r}\right)^n\right)\right) \tag{19}$$

$$0 = \frac{1}{r}\frac{\partial}{\partial r}\left(r\frac{\partial\theta}{\partial r}\right) + \left(G_r\left(a_s\frac{\partial w}{\partial r} + b_s\left(\frac{\partial w}{\partial r}\right)^{n+1}\right)\right) \tag{20}$$

3. Solution of the Problem

The exact solution of nonlinear equations (19) and (20) given by using perturbation method

$$\left.\begin{aligned} w &= w_0 + b_s w_1 \\ p &= p_0 + b_s p_1 \\ \theta &= \theta_0 + b_s\theta_1 \end{aligned}\right\} \tag{21}$$

Substituting equation (21) in equations (19)-(20) and using boundary conditions (16) we get

$$w(r,z) = \left(\frac{1}{4}k_0\left(r^2 - h^2\right) + k_1\right) + b_s\left(\frac{k_2 r^2}{4} - \frac{2^{-2-n}}{a_s(1+n)}\left(4r(k_0 r)^n - 4h(hk_0)^n + 2^n h^2 k_2 a_s(1+n)\right)\right) \tag{22}$$

$$\frac{dp}{dz} = A_1 + \frac{b_s}{a_s(1+n)}\left(A_2 + 2^{-n}r(A_1 r)^n - 2^{-n}h(A_1 h)^n\right) \tag{23}$$

$$\begin{aligned} \theta(r,z) = {} & \frac{1}{18}\left(18 + k_0 a_s G_r\left(h^3 - r^3\right)\right) + \frac{b_s G_r 2^{-1-n}}{9a_s(2+n)^2(3+n)^2} \\ & [-18h^2(hk_0)^2(3+n)^2 + a_s h^3(2+n)^2(a_s k_0(hk_0)^n + 2^n k_2(3+n)^2) \\ & + r^2(18(3+n)^2(k_0 r)^n + a_s r(2+n)^2(-2^n k_2(3+n)^2 - 9k_0(k_0 r)^n)] \end{aligned} \tag{24}$$

Where

$$\left.\begin{aligned} A_1 &= \frac{4a_s}{r^2 - h^2}(w_0 - k_1),\ \ h = 1 + \varepsilon\cos(2\pi z),\ \ k_o = \frac{1}{a_s}\frac{\partial p_o}{\partial z}, \\ k_1 &= -1 - 2\pi\varepsilon\alpha\delta\cos(2\pi z),\ \ k_2 = \frac{1}{a_s}\frac{\partial p_1}{\partial z},\ \ A_2 = \frac{4a_s(1+n)}{r^2 - h^2}(w_1) \end{aligned}\right\} \tag{25}$$

4. Results and Discussion

With a view to studied the mathematical model of peristaltic flow of Sisko fluid with heat transfer on ciliated arteries the effect of different parameters as power index n, Sisko fluid parameters a_s, b_s, the cilia length ε, eccentricity of the elliptic path α and Grashof number G_r, on the velocity, temperature and pressure gradient are illustrated through a set of Figures 2-4. In Figure 2 (a) shows the velocity profiles for different values of power index n. It is depicted that the velocity profile increases in the region $0 \le r \le 1.1$, while opposite behavior is detected when $r \rangle 1.1$. Figures 2(b) and 2(c) indicate the relation between the velocity w with Sisko fluid parameters a_s and b_s respectively. The velocity w increases with increase of b_s but decreases with increase of a_s in the region $0 \le r \le 1.1$ whereas it gets opposite behavior in the rest of the region. From Figure 2(d) the velocity profile increases with the increase of cilia length parameter ε. The variation of the velocity w for different values of the elliptic path α is shown in figure 2(e). It is shown that the velocity increases when α increase. Figures 3(a) to 3(e) reveal the variation in temperature profiles θ with varies parameters. It can be seen from figure 3(a), 3(b) and 3(c) that the temperature increases in the region $0 \le r \le 1.1$, while it is having decrease at $r \rangle 1.1$ near the wall with increasing in power index n, Sisko fluid parameter b_s and Grashof number G_r respectively. It is clear from figure 3(d) that the increases of Sisko fluid parameter a_s Mack decrease in temperature in the region $0 \le r \le 1.1$ then increase it near the wall at $r \rangle 1.1$. Figure 3(e) indicates that the increases in cilia length ε cause increase in the temperature θ. Figures 4(a) to 4(e) indicate the effects of different parameters in the pressure gradient. Figure 4(a) illustrate that the pressure gradient increases with the increase in the power index n. It is noticed that the pressure gradient decreases with increase of elliptic path α, Sisko fluid parameters b_s, and a_s respectively, observed that in Figures 4(b) to 4(d). Figure 4(e) depicts that the pressure gradient increases and decreases in different interval with increase in the cilia length ε.

5. Conclusion

In the present study, we have developed the peristaltic flow like Sisko fluid and heat transfer on ciliated arteries. The problem is simplified by using approximation of the long wavelength and low Reynolds number. Solutions have been obtained by using perturbation method. The results are illustrated analytically and graphically through a set of figures. It is observed that the velocity profile $w(r,z)$ has increases in the interval $0 \le r \le 1.1$, then decreases near the wall of the arteries at $r \rangle 1.1$ with increase of the power index n, Sisko fluid parameter b_s, While the velocity decreases in the interval $0 \le r \le 1.1$ and increases at $r \rangle 1.1$ with increase of Sisko parameter a_s. The velocity increases with increase of cilia length ε and elliptic path α. The temperature profile $\theta(r,z)$ increases in the interval $0 \le r \le 1.1$ then decreases at $r \rangle 1.1$ near the wall with increase of power index n, Sisko fluid parameter b_s and Grashof number G_r, while the temperature θ decreases in the region $0 \le r \le 1.1$ and increases at $r \rangle 1.1$ with the increase of Sisko parameter a_s. The increases of cilia length ε give increase in the temperature θ. The increases of power index n and elliptic path α get increase of the pressure gradient $(\frac{dp}{dz})$, while the increases of elliptic path α, Sisko parameters a_s and b_s give decrease the pressure gradient. The increases of cilia length ε cause increase and decrease of pressure gradient in different interval.

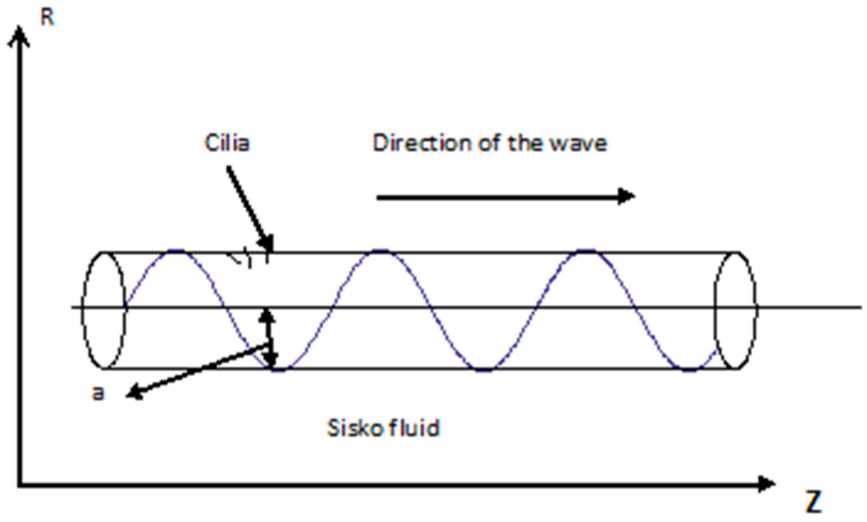

Figure 1. *Sketch of the problem.*

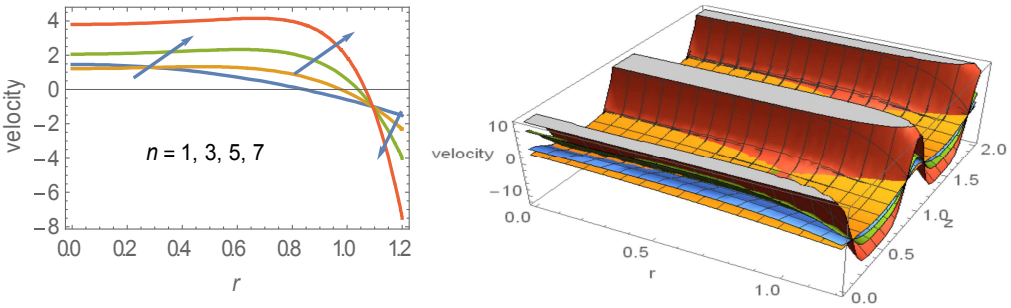

(a)

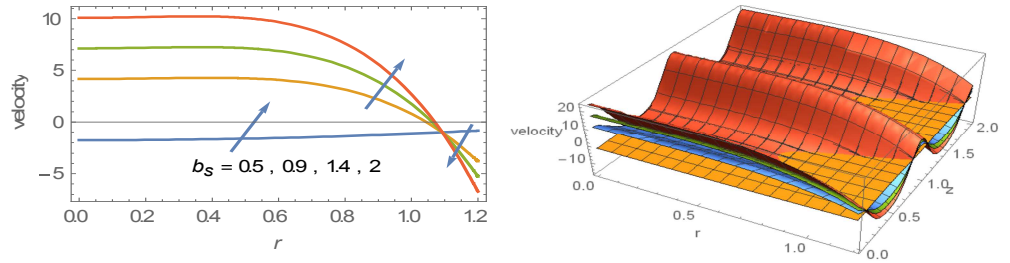

(b)

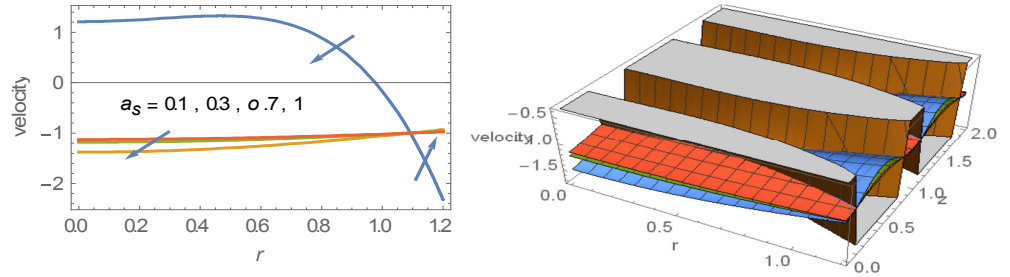

(c)

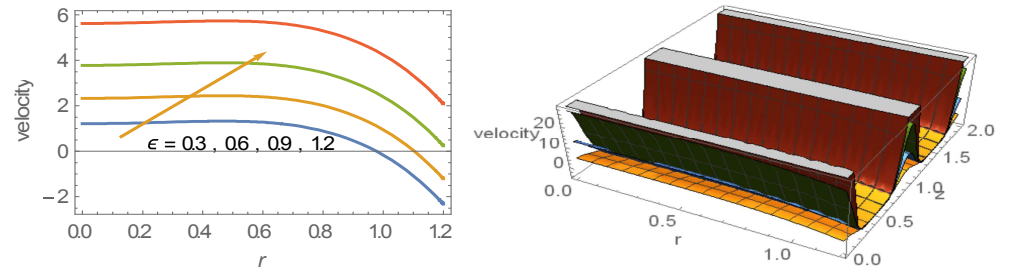

(d)

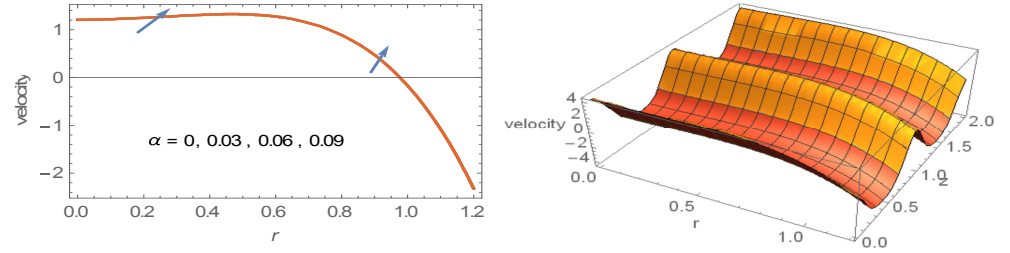

(e)

Figure 2. *a). Velocity profiles for various values of the power index* n *at* ($a_s = 0.1, b_s = 0.5, \varepsilon = 0.3, \alpha = 0.03, \delta = 0.003$). *b). Velocity profiles for various values of the Sisko fluid parameter* b_s *at* ($a_s = 0.1, n = 3, \varepsilon = 0.3, \alpha = 0.03, \delta = 0.003$). *c). Velocity profiles for various values of the sisko fluid parameter* a_s *at* ($n = 3, b_s = 0.5, \varepsilon = 0.3, \alpha = 0.03, \delta = 0.003$). *d). Velocity profiles for various values of cilia length* ε *at* ($a_s = 0.1, b_s = 0.5, n = 3, \alpha = 0.03, \delta = 0.003$) *(e). Velocity profiles for various values of the elliptic path* α *at* ($a_s = 0.1, b_s = 0.5, \varepsilon = 0.3, n = 3, \delta = 0.003$).

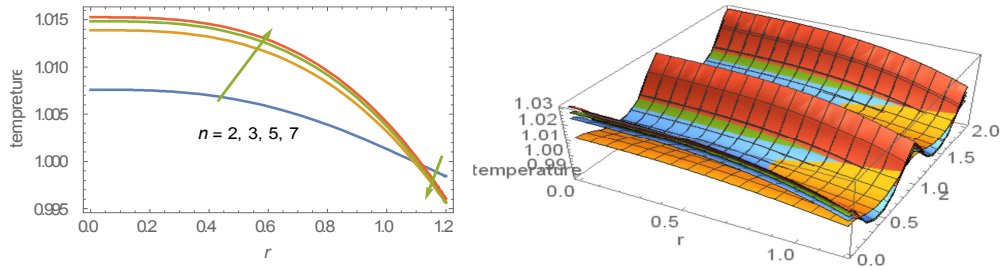

(a)

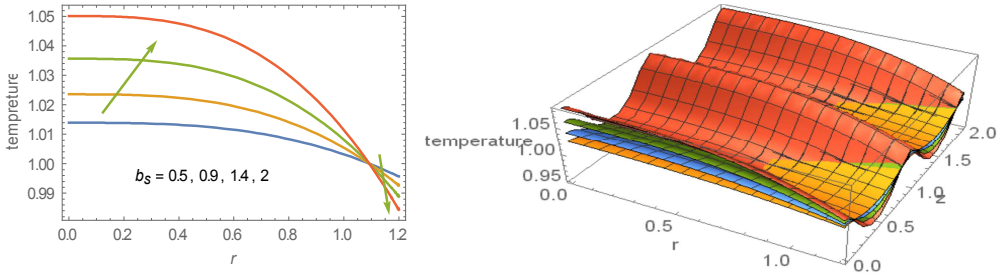

(b)

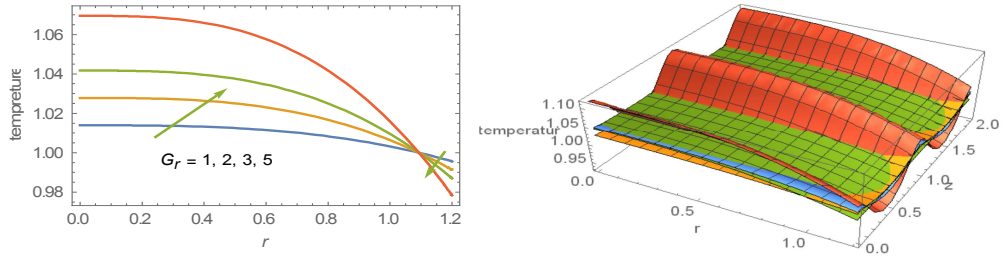

(c)

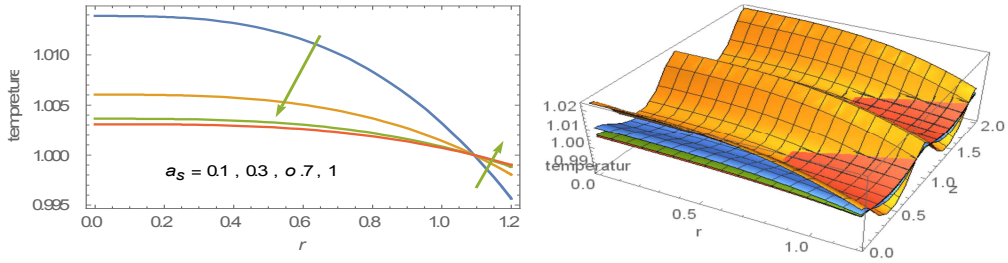

(d)

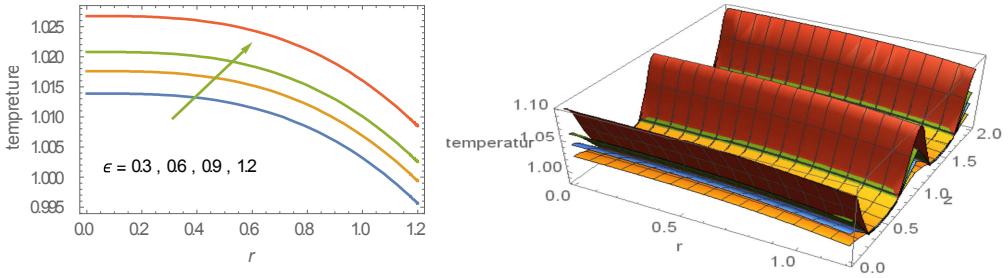

(e)

Figure 3. *a). Temperature profiles for various values of the power index* n *at* ($a_s = 0.1, b_s = 0.5, \varepsilon = 0.3, G_r = 1, \delta = 0.003$). *b). Temperature profiles for various values of the Sisko fluid parameter* b_s *at* ($a_s = 0.1, n = 3, \varepsilon = 0.3, G_r = 1, \delta = 0.003$). *c). Temperature profiles for various values Grashof number* G_r *at* ($a_s = 0.1, b_s = 0.5, \varepsilon = 0.3, n = 3, \delta = 0.003$). *d). Temperature profiles for various values of the sisko fluid parameter* a_s *at* ($n = 3, b_s = 0.5, \varepsilon = 0.3, G_r = 1, \delta = 0.003$). *e). Temperature profiles for various values of cilia length* ε *at* ($a_s = 0.1, b_s = 0.5, n = 3, G_r = 1, \delta = 0.003$).

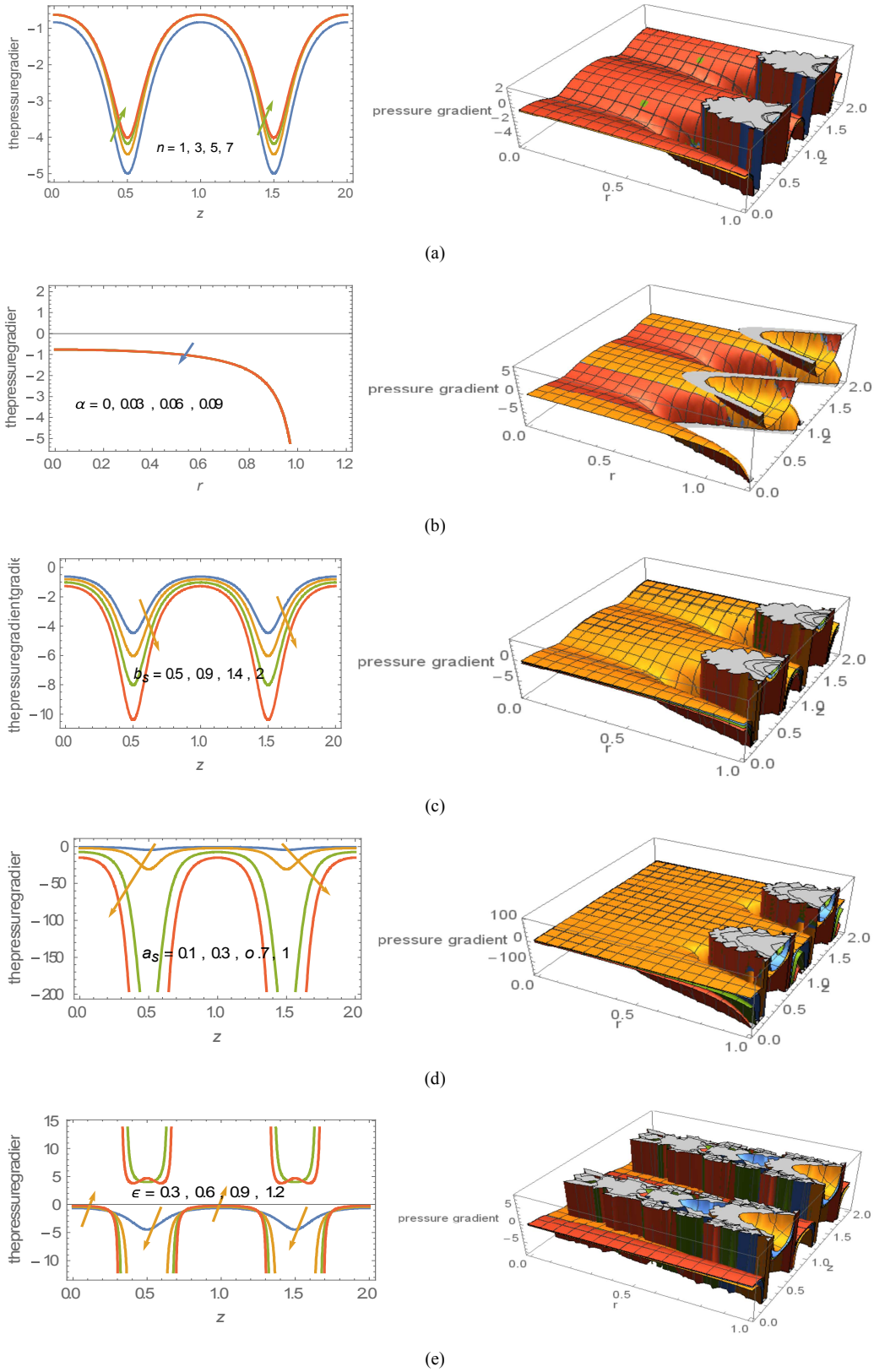

Figure 4. *a). Pressure gradient profiles for various values of the power index* n *at* $(a_s = 0.1, b_s = 0.5, \varepsilon = 0.3, \alpha = 0.03, \delta = 0.003)$. *b). Pressure gradient profiles for various values of the elliptic path* α *at* $(a_s = 0.1, b_s = 0.5, \varepsilon = 0.3, n = 3, \delta = 0.003)$. *c). Pressure gradient profiles for various values of the sisko fluid parameter* b_S *at* $(a_s = 0.1, n = 3, \varepsilon = 0.3, \alpha = 0.03, \delta = 0.003)$. *d). Pressure gradient profiles for various values of the sisko fluid parameter* a_s *at* $(n = 3, b_S = 0.5, \varepsilon = 0.3, \alpha = 0.03, \delta = 0.003)$. *e). Pressure gradient profiles for various values of cilia length* ε *at* $(a_s = 0.1, b_S = 0.5, n = 3, \alpha = 0.03, \delta = 0.003)$.

References

[1] ST. Christensen, LB. Pedersen, L. Schneider, and P Satir (2007) Sensory cilia and integration of signal transduction in human health and disease, Traffic 8, 97.

[2] JT. Eggenschwiler, and KV. Anderson (2007) Cilia and developmental Signaling, Annu Rev cell Dev Biol 23, 345.

[3] II. Banz-tallon, N. Heintz and Homran (2003) To beat or not to beat: roles of cilia in development and disease, Hum Mol Genet 12 (space no. 1), R27-35.

[4] EE. Davis, M. Brueckner, and N. Katsanis (2006) The emerging complexity of the vertebrate cilium: new functional roles for an ancient organelle, Dev Cell 11, 9.

[5] H. L Agrawal and Anawar uddin (1984) Cilia transport of bio fluid with variable viscosity, Indian J. pure apple. math. 15, 1128.

[6] S. Nadeem and H. Sadaf (2015) Metachronal wave of cilia transport in a curved channel, Zeitschrift fur Naturforschung A. 70, 33.

[7] S. Nadeem and N. S. Akbar (2010) Influence of temperature dependent viscosity on peristaltic transport of Newtonian fluid: application of an endoscope, Apple. math. comput. 216, 3606.

[8] D. Tripathi (2011) Peristaltic transport of fractional Maxwell fluids in uniform tubes: applictions in endoscopy, Comput. math. apple. 62, 1116.

[9] Kh. S. Mekheimer and Y. Abd Elmaboud (2008) Peristaltic flow of couple stress fluid in an annulus: a pplication of endoscope, Physic. A387, 2403.

[10] S. Nadeem and Hina Sadaf (2015) Trapping study of nanofluid in an annulus with cilia, Citation: Aip Advances 5, 127204.

[11] A. Shaheen and S. Nadeem (2017) Metachronal wave analysis for non-Newtonian fluid inside a symmetrical channel with ciliated Walls, Results phy. 7, 1549.

[12] R. E. Abo-Elkhair et al. (2017) Cilia walls influence on peristaltically induced motion of magneto- fluid through a porous medium at moderate Reynolds number numerical study, Journal of the Egyptian mathematical society.

[13] C. Marrase, J. H. Costello, T. Granata and J. R. Strickler (1990) Grazing in a turbulent environment: energy dissipation, encounter rates and efficacy of feeding currents incentropages humatus, proc. NatiAcad. Sci. USA 87, 1653-1657.

[14] W. Gilpin, V. N. Prakash and M. Prakash (2016) Vortex arrays and ciliary tangles underlie the feeding- swimming tradeoff in starfish larve, Nat-phys. 13, 380-386.

[15] B. A. Afzelius (1961) The fine structure of the cilia from ctenophore swimming- plates, J. Cell Biol. 9, 383-394.

[16] T. W. Lathem (1966) Fluid motion in peristaltic pump, Master's thesis Massachusetts MTT, Cambridge.

[17] V. P. Srivastava and M. Saxena (1995) Two-fluid model of non-Newtonian blood flow induced by peristaltic waves, Rheol. acta. 34, 406- 414.

[18] G. Sucharitha, S. Sreenadh and P. Lakshminarayana (2012) Peristaltic flow Of non-Newtonian fluids in an asymmetric channel with porous medium, Int. J. of Eng. Research and technology, 1 (10), 1-10.

[19] S. Sreenadh, P. Lakshminarayana and G. Sucharitha (2011) Peristaltic flow of micropolar fluid in an asymmetric channel with permeable walls, Int. J. of Appl. Math., 7, 18-37.

[20] P. Lakshminarayana, S. Sreenadh, G. Sucharitha and K. Nandagopal (2015) Effect of slip and heat transfer on peristaltic transport of a Jeffrey fluid in avertical a symmetric porous channel, Adv. Appl. Sci. Res., 6 (2): 107-118.

[21] S. Ravikumar (2016) MHD peristaltic transportation of conducting blood flow with porous medium through inclined coaxial vertical channel, In. J. of Bio- Science and Bio-Technology, Vol. 8, No. 1, pp. 11-26.

[22] S. maiti, J. C. Misra (2012) peristaltic transport of a couple stress fluid: some applications to hemodynamics, Physics. flu-dyn.

[23] A. Shaheen and MI. Asjad (2018) peristaltic flow of sisko fluid over a convectively heated surface with viscous dissipation, J. Appl. Compute Math. Vol. 7: 3.

[24] AR. Haghighi, S. Asadi Chalak (2017) Mathematical modeling of Sisko fluid flow through a stenosed artery, Int. J. Industrial Math. Vol. 9, No. 1.

[25] G. Sari, M. Pakdemirli, T. Hayat and Y. Aksoy (2012) Boundary layer equations and lie group analysis of sisko fluid, Journal of applied mathematics.

[26] S. Nadeem and N. S. Akbar (2010) Peristaltic flow of sisko fluid in a uniform inclined tube, Acta Mach Sin.

[27] N. S. Akbar (2014) Peristaltic sisko nano fluid in an asymmetric channel, App. Nanosci.